Syukuro Manabe, Ronald J. Stouffer and Michael J. Spelman

Response of a Coupled Ocean-Atmosphere Model to Increasing Atmospheric Carbon Dioxide

This study investigates the response of a climate model to a 1% per year increase of atmospheric carbon dioxide. The model is a general circulation model of the coupled ocean-atmosphere-land surface system, with a global computational domain, smoothed geography, and seasonal variation of insolation. The simulated increase of sea-surface temperature is very slow in the northern North Atlantic and the Circumpolar Ocean of the Southern Hemisphere where the vertical mixing of water penetrates very deeply and the rate of deep water formation is relatively fast. Extending this work, we investigated the transient responses of the coupled model to the doubling and quadrupling of atmospheric CO_2, over the period of several centuries. During the entire 500-yr period of the experiment, the global mean surface air temperature increases almost 3.5°C when CO_2 is doubled, and 7°C when it is quadrupled. In the latter experiment, the thermal structure and dynamics of the model oceans undergo drastic changes, such as cessation of the thermohaline circulation in most of the model oceans, and substantial deepening of the thermocline, especially in the North Atlantic. These changes prevent the ventilation of the deeper layer of the oceans and, if they occurred in reality, could have a profound impact on the carbon cycle and biogeochemistry of the coupled ocean-atmosphere system.

INTRODUCTION

The interactions among the atmosphere, oceans and land surface play a major role in determining the future climate change induced by greenhouse gases. The CO_2-induced change of climate has been the subject of many studies by use of general circulation models of the coupled ocean-atmosphere-land surface system (1–13).

This paper describes the response of a coupled ocean-atmosphere-land surface model, developed at the Geophysical Fluid Dynamics Laboratory, to increasing atmospheric CO_2. It includes a summary of the results in three published papers (9, 11, 12). In addition, results from recent investigations (14, 15) are discussed, exploring the multiple-century response of the coupled model to a doubling and quadrupling of atmospheric CO_2.

In response to an increase of atmospheric CO_2, the infrared opacity of the atmosphere increases, thereby raising the effective source of emission for the outgoing terrestrial radiation (at the top of the atmosphere) to a higher level which has lower temperature. This upward shift of the effective emission source results in warming of both the convective troposphere and the Earth's surface, which are coupled closely to each other by the efficient boundary-layer heat exchange. The rise of tropospheric temperature, in turn, induces an increase of the moisture content of air, further enhancing the infrared opacity of the atmosphere

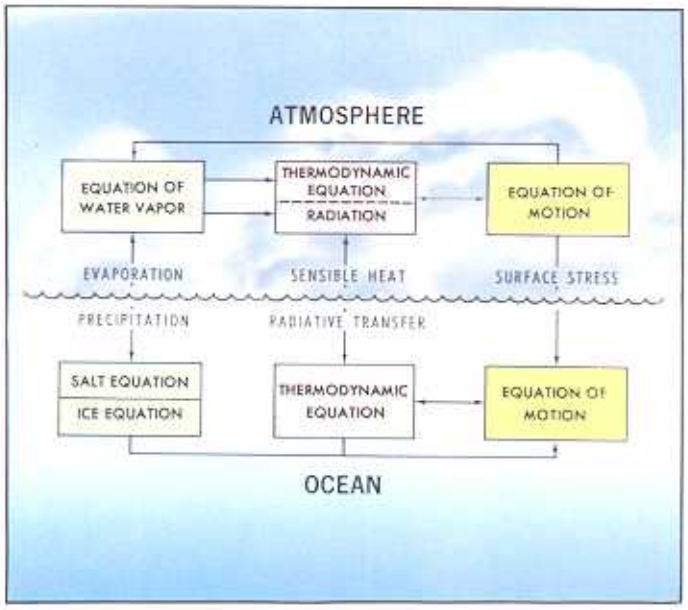

Figure 1. Illustration of coupling between the oceanic and atmospheric components of the model.

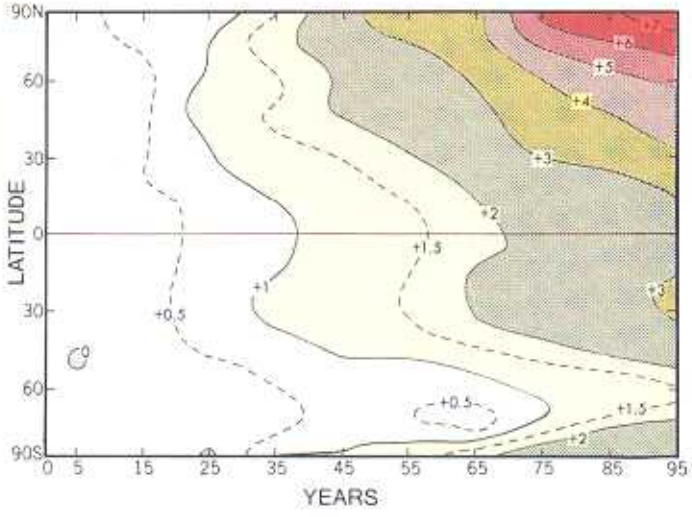

Figure 2. Latitude-time distribution over 100 yr for the difference in zonally averaged decadal mean surface air temperature (°C) between the standard integration of the coupled ocean-atmosphere model, with unchanged, present-day levels of CO_2, and the integration for CO_2 increases of 1% per year (11).

Figure 3. The latitudinal distribution of the difference in zonal mean temperature (°C) of the coupled model between the standard and CO_2-growth integrations, shown as a function of atmospheric height and ocean depth, for the 60–80th yr period of the experiment. When the atmospheric CO_2 is doubled in the CO_2 growth simulation.

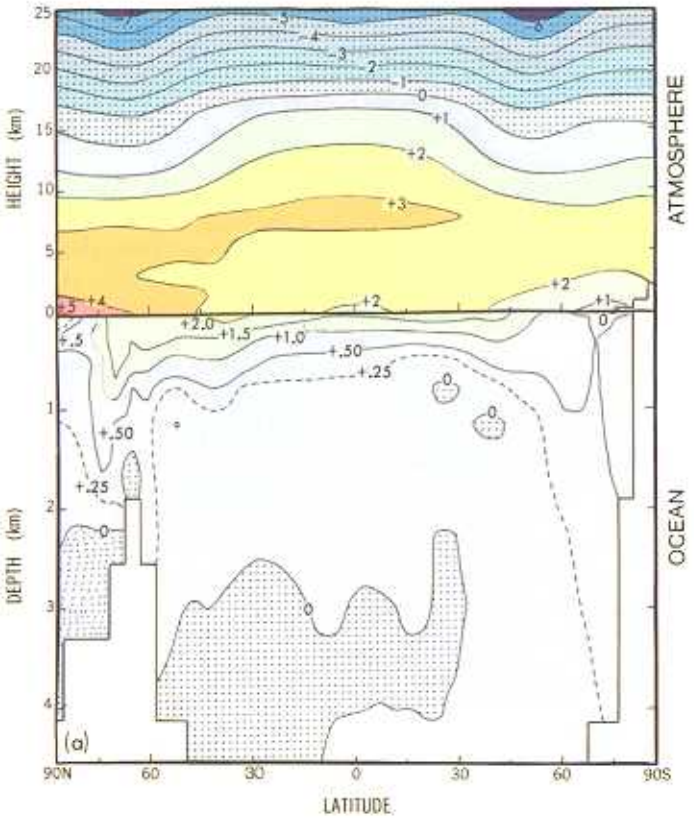

and further raising the temperature of the troposphere-surface system (16).

The warming of the coupled system is reduced by the effective thermal inertia of the oceans, which is essentially controlled by the vertical mixing of heat in the oceans. This study describes how such vertical mixing of heat delays the greenhouse warming in the coupled troposphere-ocean-land surface system.

MODEL STRUCTURE

The model consists of general circulation models (GCM) of the atmosphere and oceans, and a simple model of the continental surface that involves the budgets of heat and water (17). It is a global model with realistic geography. The atmospheric component of the model includes the seasonal variation of insolation, and predicted cloud cover which depends only on relative humidity. It has nine vertical finite difference levels. The horizontal distributions of predicted variables are represented by spherical harmonics (15 associated Legendre functions for each of 15 Fourier components) and grid-point values (18).

The ocean GCM uses a full finite difference technique and has a regular grid system with 4.5° x 3.75° (latitude x longitude) spacing and 12 vertical levels (19). The atmospheric and oceanic components of the model interact with each other continuously through the exchange of heat, water and momentum fluxes as illustrated by Figure 1. For further details of the model used here, see (11).

NUMERICAL EXPERIMENTS

To study the response of the coupled ocean-atmosphere-land surface model to a gradual increase of atmospheric carbon dioxide, two 100-yr integrations were performed. Starting from an initial condition in a quasi-equilibrium state, the standard time integration of the coupled model was performed with the normal concentration of atmospheric carbon dioxide. In the other integration, the CO_2 concentration was increased by 1% per yr (compounded). The rate of 1% per yr is chosen because the total CO_2-equivalent amount of various greenhouse gases, other than water vapor, is currently increasing at approximately this rate (20).

The initial conditions for both integrations have realistic seasonal and geographical distributions of surface temperature, surface salinity, and sea ice, with which both the atmospheric and oceanic components of the model are nearly in equilibrium. This quasi-equilibrium condition was obtained by separate time integrations of these two components of the model with observed surface boundary conditions. The convergence of the oceanic component towards equilibrium was accelerated by the method described in (21).

When the time integration of a model starts from the initial conditions identified above, the model climate undergoes a rapid drift towards its own equilibrium state. To prevent the drift, the fluxes of heat and water at the ocean-atmosphere interface are adjusted by amounts that vary seasonally and geographically (11). These adjustments do not change from one year to the next and are independent of the anomalies of temperature and salinity at the oceanic surface. Thus, they neither damp nor amplify the anomalies.

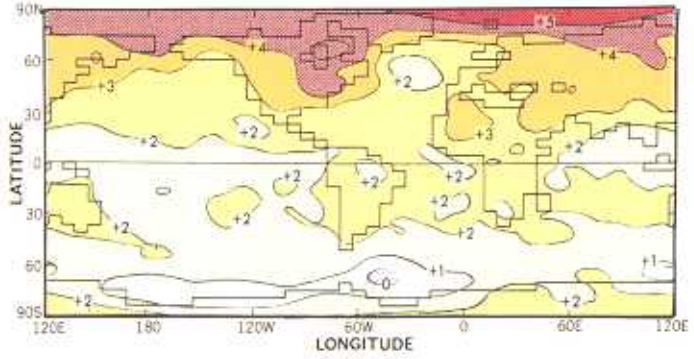

Figure 4. The geographical distribution of the difference in surface-air temperature (°C) between the standard and CO_2 growth integrations, shown as the average over the 60–80th yr period of the experiment when atmospheric CO_2 is doubled.

TEMPERATURE CHANGE

Annual Mean Response

Figure 2 shows the latitude-time distribution of the CO_2-induced change of zonally averaged, decadal-mean surface-air temperature during the 100 yr experiment. In the Northern Hemisphere the warming of surface air increases with latitude, partly because of the poleward retreat of both snow cover and sea ice, which have high surface albedo. The relatively large warming in high northern

latitudes is essentially confined to the lower troposphere because of the stable stratification. This is indicated in Figure 3, which shows, for both the atmosphere and oceans, the zonal-mean temperature difference between the two integrations for the 20-yr period between the 60–80th years of the experiment. The oceanic warming is essentially confined to the upper layers, except near Antarctica and around 70° N.

The simulated response of surface air temperature is relatively small over the Circumpolar Ocean of the Southern Hemisphere and the northern North Atlantic (Fig. 4). As explained in (11), the vertical mixing of water extends very deeply in these regions through vertical subgrid-scale mixing including convection. Because of this deep vertical mixing, heat sequestered by the increasing atmospheric carbon dioxide spreads over a thick layer of water, thereby making the warming of surface temperature very small in these oceanic regions.

In both the northern North Atlantic and the Circumpolar Ocean of the Southern Hemisphere, there are other physical mechanisms that reduce the CO_2-induced increase of sea surface temperature. For example, the surface warming in the North Atlantic is reduced further because the northward advection of warm surface water decreases due to the weakening of the thermohaline circulation. This effect is described in more detail below, under Multiple-Century Responses; also see (11) for additional elucidation of these processes.

Seasonal Dependence

In response to a gradual increase of atmospheric CO_2, the increase of surface air temperature is at a maximum over the Arctic Ocean and its surroundings in late autumn and winter. On the other hand, the Arctic warming is at a minimum in summer (Fig. 5). The mechanism responsible for the seasonal dependence of the Arctic surface-air temperature change is similar to the mechanism noted in an equilibrium experiment which was conducted earlier (23, 24) with an atmospheric GCM coupled with a mixed-layer ocean model. Because of the existence of a halocline with very stable stratification, the heat exchange between the mixed layer and deeper ocean is very small in the Arctic Ocean. Therefore, it is not surprising that the seasonal variation of CO_2-induced change in surface air temperature obtained from the present model is qualitatively similar to the response of a coupled atmosphere mixed-layer ocean model.

The results from the present and earlier studies (23, 24) indicate that, during autumn and winter, the large increase of surface air temperature is achieved by the enhanced upward heat conduction from the ocean to the cold, overlying atmosphere through thinner sea ice. During the warm season, the downward flux of terrestrial radiation increases in response to the increase of greenhouse gases (i.e., CO_2 and H_2O) in the atmosphere, and the reflection of solar radiation by the surface decreases due to the reduced coverage of sea ice, enhancing the absorption of radiative energy by the mixed layer of ocean. However, the temperature of the sea surface and overlying air hardly changes in summer because they are anchored near the freezing point due to the melting of sea ice. The additional heat, which is thus stored in the mixed layer of ocean during the warm season, is lost to the atmosphere during the cold season due to the enhanced heat conduction through thinner sea ice, thereby increasing surface air temperature.

In sharp contrast to the situation in the Arctic Ocean, the increase of surface air temperature and its seasonal variation in the Circumpolar Ocean of the Southern Hemisphere are very small

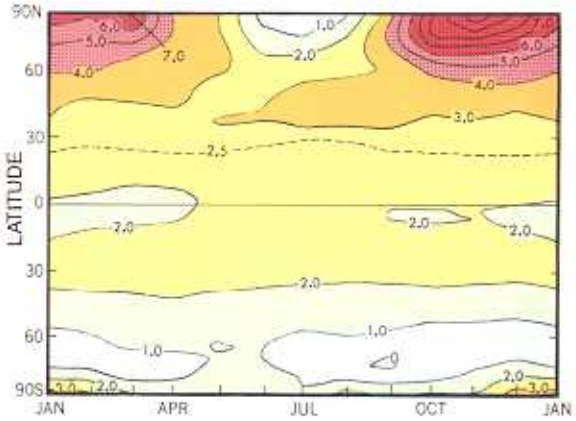

Figure 5. Seasonal and latitudinal variation of the difference in zonal mean surface air temperature (°C) between the standard and CO_2-growth integrations, shown as the average over the 60–80th yr period when atmospheric CO_2 is doubled.

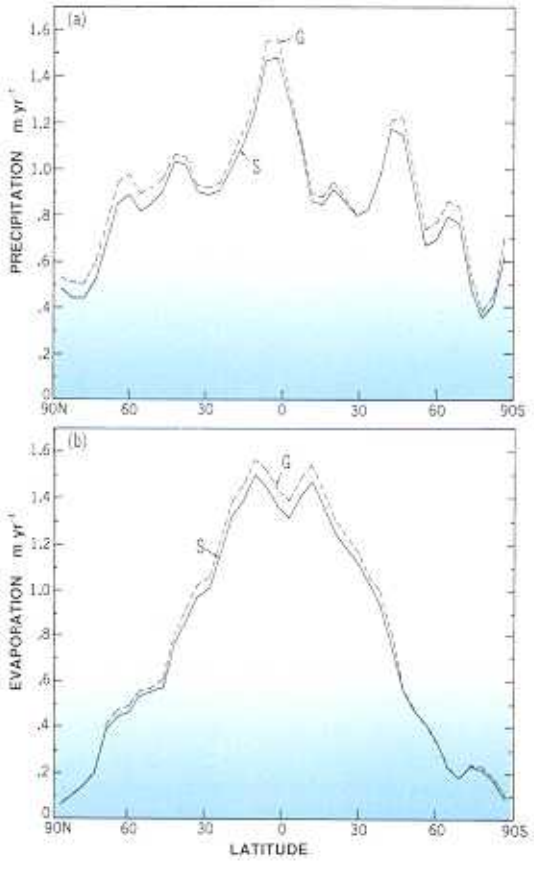

Figure 6. The latitudinal profiles of zonal mean rates of precipitation (a), and evaporation (b), averaged over the 60–80th yr period of the experiment (11). Solid line, standard integration (S); dashed line, CO_2-growth integration (G).

due to the deep vertical mixing of water discussed earlier. Thus the maximum warming during the cold season does not materialize in the Circumpolar Ocean. This is quite different from the results of the earlier equilibrium experiments conducted by use of a coupled atmosphere mixed-layer ocean model.

HYDROLOGICAL CHANGES

Figure 6 illustrates the CO_2-induced change in the zonal mean rates of precipitation and evaporation averaged over the 60–80th year period of the experiment. This figure indicates that, as noted in many previous studies (e.g. 25) the annual mean rates of both precipitation and evaporation increase as the result of an increase of atmospheric carbon dioxide. However, the latitudinal profile of the CO_2-induced increase in precipitation rate is quite different from the latitudinal profile of evaporation increase. In general, the change in evaporation decreases with increasing latitudes and is very small in high latitudes. On the other hand, the enrichment of water vapor in air accompanying the warming enhances the poleward moisture transport in the atmosphere, thereby causing a substantial increase in the precipitation rate in high latitudes. Thus, the excess of precipitation over evaporation also increases significantly in these latitudes and contributes to the marked increase in river runoff in the subarctic regions.

It is notable that, in the present experiment, the precipitation rate increases even in high latitudes of the Southern Hemisphere where the CO_2-induced surface warming is small. As indicated in Figure 3, significant mid-tropospheric warming occurs in high latitudes of the Southern Hemisphere, thereby enhancing the penetration of warm, moisture-rich air towards the Antarctic continent.

The CO_2-induced changes in the annual mean rates of precipitation and evaporation described above increase the excess of precipitation over evaporation in high latitudes, thereby reducing the salinity in the upper layer of the model ocean. The capping of the Atlantic Ocean by water of relatively low salinity weakens the thermohaline circulation, moderating the increase of surface-air temperature in the northern North Atlantic (9, 11, 12). This topic is discussed further in the following section.

MULTIPLE-CENTURY RESPONSES

In order to assess the possible future change of climate over the next several centuries, the numerical integrations of the coupled model are extended to 500 yr (14, 15). In addition to the standard integration (S) in which the atmospheric CO_2 remains unchanged, two further integrations are conducted (Fig. 7a). In one integration, (2XC), the atmospheric CO_2 concentration increases by 1%

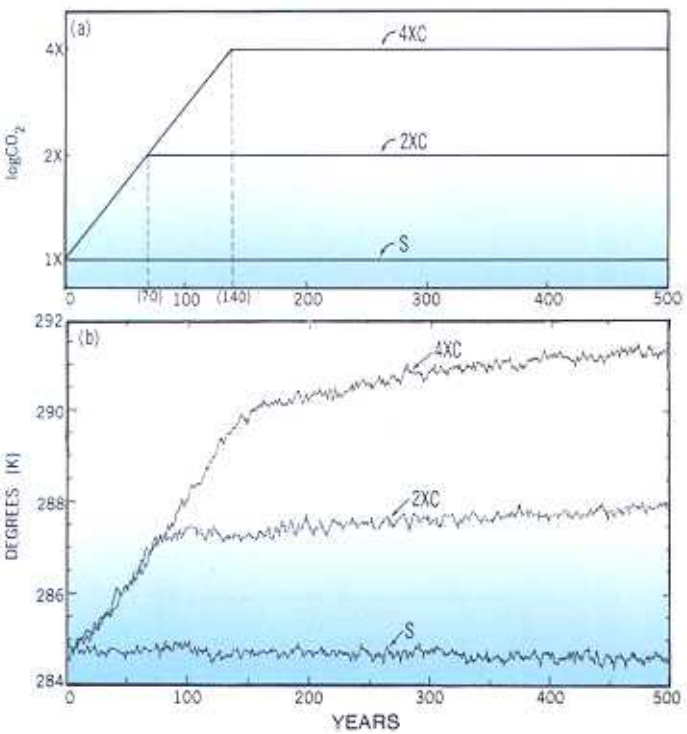

Figure 7. Changes over the 500-yr experimental period of (a) logarithm of atmospheric CO_2 concentration, and (b) global mean surface air temperature (° K), computed as the differences between the standard integration (S) and those for doubled (2XC) and quadrupled (4XC) CO_2 (14).

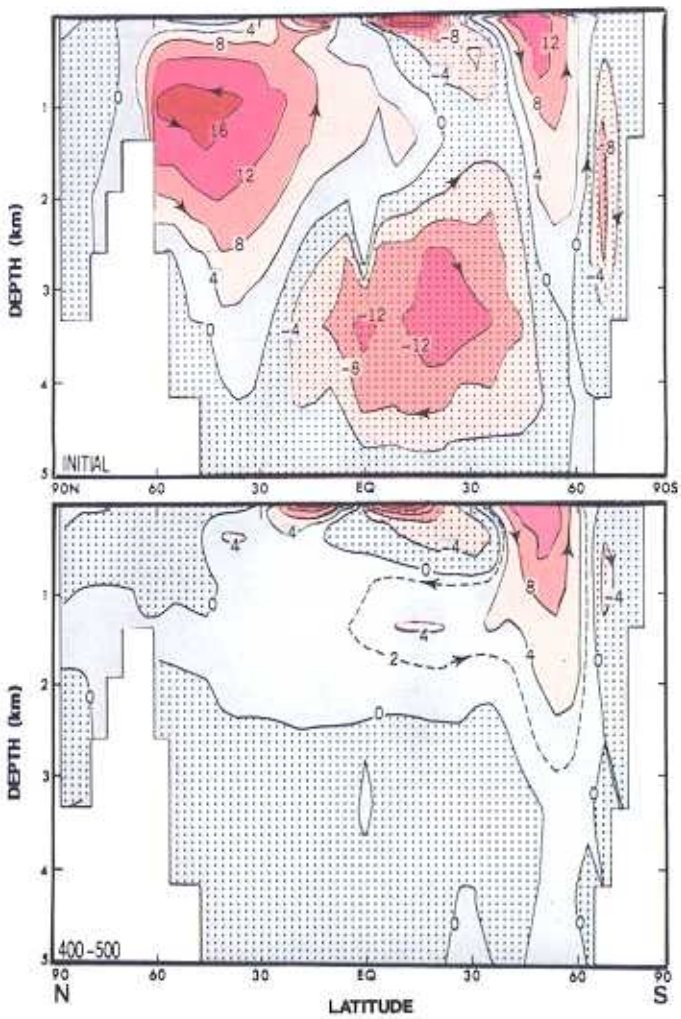

Figure 8. Stream function of zonal mean meridional circulation in the model oceans (14). Top: initial distribution obtained from the standard integration. Bottom: average over the 400–500th yr of the quadrupled CO_2 integration. Units are Sverdrups (10^6 m^3 sec^{-1}).

per yr (compounded) until it reaches twice the initial value around the 70th year and remains unchanged thereafter. In the other integration, (4XC), the CO_2 concentration also increases by 1% per yr until it reaches four times the initial value at the 140th year and remains unchanged thereafter. By comparing these three integrations, one can evaluate the long-term impact of the eventual doubling or quadrupling of atmospheric CO_2 upon the global climate system.

Figure 7b shows the time series of global mean surface-air temperature from the S, 2XC and 4XC integrations. During the first 140 yr of the 4XC integration, the global mean surface air temperature increases at the rate of approximately 3.5° C per century. After the 140th year, global mean surface air temperature increases slowly by an additional 1.5°C despite the absence of further CO_2 increase in the model atmosphere. Over the entire 500-year period, the global mean surface air temperature increases by 7°C and the thermocline becomes deeper, particularly over the Atlantic Ocean.

A qualitatively similar behavior is evident in the temporal variation of global mean surface air temperature from the 2XC integration. During the first 70 yr, the global mean temperature increases by 2.5°C, again at the rate of about 3.5°C per century. After atmospheric CO_2 stops increasing at the 70th yr, the global mean surface air temperature increases by an additional 1°C.

One of the most notable features of the 4XC experiment is the gradual disappearance of thermohaline circulations in most of the model oceans during the first 250 yr period, leaving behind only surface wind-driven cells (Fig. 8). For example, the thermohaline circulation nearly vanishes in the North Atlantic during the first 200 years of the integration (Fig. 9). In the immediate vicinity of the Antarctic Continent the thermohaline circulation becomes weaker and shallower (Fig. 8) markedly reducing the formation of Antarctic Bottom Water. This, in turn, weakens the northward flow of bottom water in the Pacific and Atlantic Oceans.

The near extinction of the thermohaline circulation described above is attributable mainly to the capping of the model oceans by relatively fresh water where the supply of water to the ocean surface increases markedly. The excess of precipitation over evaporation and runoff from continents increases in high latitude due to the enhanced poleward transport of water vapor in the warmer model troposphere, as discussed in the previous section.

In the 2XC experiment, the intensity of the thermohaline circulation also keeps decreasing in the North Atlantic long after the 70th yr, when atmospheric carbon dioxide stops increasing and the rate of surface warming and freshening are reduced abruptly. It eventually is reduced to less than half of its original intensity (Fig. 9). However, the thermohaline circulation begins to intensify very slowly around the 150th year of the integration. Because of the reduction of the upward advection of cold water that accompanies the weakening of the thermohaline circulation in low latitudes, a large warming of the subsurface layer takes place in the 2XC integration between the equator and 45°N latitude. The resulting increase in the density contrast between the sinking and rising regions in the North Atlantic overshadows the salinity-induced reduction in density contrast and appears to be responsible for the gradual re-intensification of the thermohaline circualtion in the North Atlantic by the 500th yr. This intensification is aided by the gradual increase and recovery of salinity toward the initial value, due to the enhanced northward advection of saline water by the thermohaline circulation.

The results from the 2XC integration described above imply that the weakening of the thermohaline circulation in the Atlantic during the early phases of both experiments is not the collapse of the circulation due to an instability. Instead, it represents the slow adjustment of the circulation to the evolving density structure of the model's Atlantic Ocean. However, the thermohaline circulation eventually collapses in the 4XC integration, and does not regenerate despite the downward penetration of positive temperature anomaly in low and middle latitudes of the North Atlantic. This suggests that the state of inactive thermohaline circulation reached in the 4XC integration is a stable state which is distinct from the state of the active circulation maintained in the early phase of both

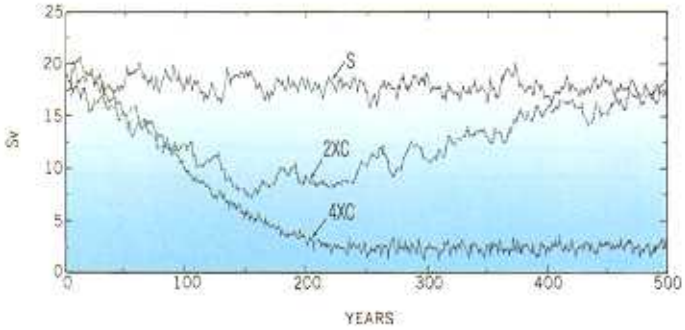

Figure 9. Temporal variation of the intensity of the thermohaline circulation in the North Atlantic Ocean from the standard (S), doubled (2XC) and quadrupled (4XC) CO_2 integrations (14). Here, the intensity is defined as the maximum value of stream function, in Sverdrups, representing the meridional circulation in the North Atlantic Ocean.

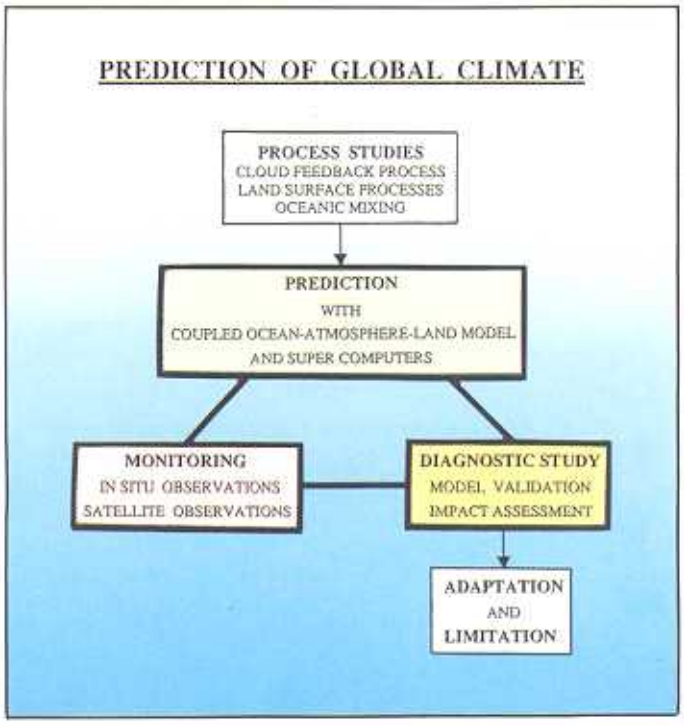

Figure 10. The triad strategy for the monitoring and prediction of inter-decadal climate change.

integrations. The existence of two stable equilibria in a coupled ocean atmosphere model has been demonstrated previously (26).

In summary, this study explores the responses of a coupled model to both doubling and quadrupling of atmospheric CO_2 over the period of several centuries. During the entire 500-yr periods of these two experiments, the global mean surface air temperature increases by almost 3.5° and 7.5°C, respectively. In the CO_2-quadrupling experiment, the warming is almost as large as the difference between the present climate and the very warm climate of the late Cretaceous (27, 28). Furthermore, the thermal and dynamical structure of the model oceans undergoes drastic changes, such as the cessation of thermohaline circulation in most of the model oceans, and a substantial deepening of the thermocline, especially in the North Atlantic. These changes prevent the ventilation of the deep ocean and could have a profound impact on the carbon cycle and biogeochemistry of the coupled system.

Averaged over the entire globe, the rate of increase in surface-air temperature is approximately 3.5°C per century during the first 150 years of the CO_2-quadrupling integration, in response to an increase of atmospheric concentration of CO_2 at the rate of 1% per yr. This rate of increase in CO_2 is approximately equal to the business-as-usual scenario for the rate of increase of CO_2-equivalent greenhouse gases, as estimated by the 1990 Scientific Assessment of the Intergovernmental Panel on Climate Change (22). The temperature response is slightly larger than the rate of 3.0°C per century which is the best estimate by the IPCC for the business-as-usual case. It has also been estimated that the equilibrium response of the present model to the doubling of atmospheric CO_2 is approximately 3.5°C in global mean surface air temperature. This response belongs in the upper half of the 1.5–4.5° C range of climate sensitivity estimated by the IPCC. Thus, it is possible that the present model exaggerates somewhat the sensitivity of actual climate.

According to the IPCC (22), the quadrupling of the CO_2-equivalent of greenhouse gases could be realized if the business-as-usual emission of greenhouse gases continues until the end of the 21st century. Draconian measures would probably be required to prevent the CO_2 equivalent of greenhouse gases from quadrupling during the next several centuries (29). Considering the possible overestimate of climate sensitivity by the present model, it may be reasonable to speculate that the CO_2-doubling and quadrupling experiments provide a probable range of future climate change. Thus, one should not discard too readily the possibility of a very large long-term climate change such as that which occurred in the CO_2-quadrupling experiment.

LONG-TERM MONITORING OF THE COUPLED SYSTEM

The future climate changes obtained in the present study are subject to large uncertainties because of our inability to model various processes that control future climate change. It is therefore necessary to improve various components of the climate model, such as the cloud feedback and land surface processes. In addition, it is essential to carefully assess the model predictions of future climate change based upon the reliable, long-term monitoring of climate forcing factors and actual climate changes. The agreement between the simulated and observed climate should enhance our confidence in model prediction. A comprehensive triad strategy for predicting future climate is illustrated in Figure 10. It involves the monitoring of the coupled ocean-atmosphere-land surface system by *in situ* and remote sensing, the prediction of future climate by state-of-the-art models, and in-depth analysis of predicted and monitored climate. The insight gained by this comprehensive effort is indispensable not only for enhancing our confidence in model prediction of future climate, but also for adapting to future climate change and limiting the emission of greenhouse gases.

References and Notes

1. Bryan, K., Komro, F.G., Manabe, S. and Spelman, M.J. 1982. Interhemispheric asymmetry in the transient response to increasing atmospheric carbon dioxide. *Science 21*, 56–58.
2. Spelman, M.J. and Manabe, S. 1984. Influence of oceanic heat transport upon the sensitivity of a model climate. *J. Geophys. Res. 89*, 571–586.
3. Schlesinger, M.E., Gates, W.L. and Han, Y.J. 1985. The role of the ocean in CO_2-induced climatic warming: Preliminary results from the OSU coupled atmosphere-ocean GCM. In: *Coupled Ocean-Atmosphere Models*. Nihoul, J.C.J. (ed.). Elsevier, New York, p. 447–478.
4. Bryan, K. and Spelman, M.J. 1985. The ocean's response to a carbon dioxide-induced warming. *J. Geophys. Res. 90 (C6)*, 11 679–11 688.
5. Bryan, K., Manabe, S. and Spelman, M.J. 1988. Interhemispheric asymmetry in the transient response of a coupled ocean-atmospheric model to a CO_2 forcing. *J. Phys. Oceanogr. 18*, 851–867.
6. Schlesinger, M.E. and Jiang, X. 1988. The transport of CO_2-induced warming into the ocean: An analysis of simulations by the OSU coupled atmosphere-ocean general circulation model. *Climate Dynamics 3*, 1–17.
7. Hansen, J., Fung, I., Lacis, A., Rind, D., Lebedeff, S., Roedy, R., Russell, G. and Stone, P. 1988. Global climate change as forecast by Goddard Institute for Space Studies three-dimensional models. *J. Geophys. Res. 93*, 9341–9364.
8. Washington, W.M. and Meehl, G.A. 1989. Climate sensitivity due to increased CO_2: Experiment with a coupled atmosphere and ocean general circulation model. *Climate Dynamics 4*, 1–38.
9. Stouffer, R.J., Manabe, S. and Bryan, K. 1989. Interhemispheric asymmetry in climate response to a gradual increase of atmospheric CO_2. *Nature 342*, 660–662.
10. Manabe, S., Bryan, K. and Spelman, M.J. 1990. Transient response of a global ocean-atmosphere model to a doubling of atmospheric carbon dioxide. *J. Phys. Oceanogr. 20*, 722–749.
11. Manabe, S., Stouffer, R.J., Spelman, M.J. and Bryan, K. 1991. Transient responses of a global ocean-atmosphere model to gradual changes of atmospheric CO_2: Part I. Annual mean response. *J. Climate 4*, 785–818.
12. Manabe, S., Spelman, M.J. and Stouffer, R.J. 1992. Transient response of a coupled ocean-atmosphere model to gradual changes of atmospheric CO_2: Part II. Seasonal response. *J. Climate 5*, 105–126.
13. Cubasch, U., Hasselman, K., Hoch, H., Maier-Reimer, E., Mikolajewicz, U., Santer, B.D. and Sausen, R. 1992. Time-dependent greenhouse warming computations with a coupled ocean-atmosphere model. *Climate Dynamics 8*, 55–69.
14. Manabe, S. and Stouffer, R.J. 1993. Century-scale effect of increased atmospheric CO_2 on the ocean-atmosphere system. *Nature 364*, 215–218.
15. Manabe, S. and Stouffer, R.J. 1994. Multiple century response of a coupled ocean-atmosphere model to an increase of atmospheric carbon dioxide. *J. Climate 1*, 5–23.
16. Manabe, S. and Wetherald, R.T. 1967. Thermal equilibrium of the atmosphere with a given distribution of relative humidity. *J. Atmos. Sci. 24*, 241–259.
17. Manabe, S. 1969. Climate and the ocean circulation: I. The atmospheric circulation and the hydrology of the earth's surface. *Mon. Weather Rev. 97*, 739–774.
18. Gordon, C.T. and Stern, W. 1982. A description of the GFDL Global Spectral Model. *Mon. Weather Rev. 110*, 625–644.
19. Bryan, K. and Lewis, L.J. 1979. A water mass model of the world ocean. *J. Geophys. Res. 84 (C5)*, 2503–2517.
20. Ramanathan, V., Cicerone, R.J., Singh, H.B. and Kiehl, J.T. 1985. Trace gas trends and their potential role in climate change. *J. Geophys. Res. 90*, 5547–5566.
21. Bryan, K. 1984. Accelerating the convergence to equilibrium of ocean-climate models. *J. Phys. Oceanogr. 14*, 666–673.
22. Houghton, J.T., Jenkins, G.J. and Ephraums, J.J. (eds). 1990. *Climate Change. The IPCC Scientific Assessment*. Cambridge University Press, Cambridge.
23. Manabe, S. and Stouffer, R.J. 1979. A CO_2-climate sensitivity study with a mathematical model of the global climate. *Nature 282*, 491–493.
24. Manabe, S. and Stouffer, R.J. 1980. Sensitivity of a climate model to an increase of CO_2 concentration in the atmosphere. *J. Geophys. Res. 85 (C10)*, 5529–5554.
25. Manabe, S. and Wetherald, R.T. 1975. The effect of doubling CO_2 concentration on the climate of a general circulation model. *J. Atmos. Sci. 32*, 3–15.
26. Manabe, S. and Stouffer, R.J. 1988. Two stable equilibria of a coupled ocean-atmosphere model. *J. Climate 1*, 841–866.
27. Crowly, T.J. and North, G.N. 1991. *Palaeoclimatology*. Oxford Monograph on Geology and Geophysics. No. 16.
28. Lloyd, C.R. 1984. Pre-Pleistocene palaeoclimate: The geological and paleontological evidence: Modeling strategies, boundary conditions and some preliminary results. *Adv. Geophys. 26*, 36–140.
29. Walker, J.C.G. and Kasting, J.F. 1992. Effect on fuel and forest conservation on future level of atmospheric carbon dioxide. *Palaeogeography, Palaeoclim. Palaeoecol. (Global Planetary Change Section) 97*, 151–189.

Syukuro Manabe is group leader of the climate dynamics project of the Geophysical Fluid Dynamics Laboratory (GFDL) of the National Oceanic and Atmospheric Administration (NOAA) at Princeton University. During the past 35 years at GFDL, he has been involved in the development of climate models and their application, pioneering the modeling study of greenhouse warming. He is a member of the US National Academy of Sciences, and his academic awards include the Blue Planet Prize from the Asahi Glass Foundation, Japan, the Carl Gustaf Rossby Medal of the American Meteorological Society, and the Roger Revelle Medal of the American Geophysical Union. Ronald J. Stouffer is a senior research associate at GFDL, where he has worked since 1977. He is the chief architect of the current version of the coupled ocean-atmosphere model described in this article, and has skillfully used the model for the study of climate. Michael J. Spelman is a senior research associate at GFDL, where he has worked since 1969. His contribution has been essential for the development of many generations of coupled ocean-atmosphere models at the laboratory. Their address: Geophysical Fluid Dynamics Laboratory/NOAA, Princeton University, PO Box 308, Princeton, New Jersey 08542, USA.